



Forschungszentrum Karlsruhe
in der Helmholtz-Gemeinschaft

Wissenschaftliche Berichte
FZKA 7254

Air Shower Simulation with CORSIKA at Arbitrary Direction of Incidence

D. Heck
Institut für Kernphysik

November 2006

Forschungszentrum Karlsruhe

in der Helmholtz-Gemeinschaft

Wissenschaftliche Berichte

FZKA 7254

Air Shower Simulation with CORSIKA at Arbitrary Direction of Incidence

D. Heck

Institut für Kernphysik

Für diesen Bericht behalten wir uns alle Rechte vor

Forschungszentrum Karlsruhe GmbH
Postfach 3640, 76021 Karlsruhe

Mitglied der Hermann von Helmholtz-Gemeinschaft
Deutscher Forschungszentren (HGF)

ISSN 0947-8620

urn:nbn:de:0005-072546

Abstract

Air Shower Simulation with CORSIKA at Arbitrary Direction of Incidence

The program CORSIKA has been extended to allow the simulation of air showers at arbitrary angle of incidence. In the new version of CORSIKA, also the curved geometry of the atmosphere and upward going particles are optionally taken into account by combination of the options *CURVED* with *UPWARD*. This combination enables arbitrary angles of incidence for the primary shower particle, including the skimming incidence at any altitude of the horizontal shower axis above the detector level. In this report the action of the combination of options *CURVED*, *UPWARD* and *SLANT* of the air shower simulation program CORSIKA is described. The *SLANT* option may be combined with all other options and defines the penetration depth of the shower along the shower axis for the longitudinal development as *slant depth*, independent of the primary direction.

Zusammenfassung

Luftschauersimulation mit CORSIKA bei beliebiger Einfallrichtung

Das Programm CORSIKA wurde erweitert, um die Simulation von Luftschauern mit beliebigem Einfallswinkel zu ermöglichen. In der neuen CORSIKA-Version besteht die Möglichkeit, auch die gekrümmte Geometrie der Atmosphäre und aufwärts fliegende Sekundärteilchen gleichzeitig durch die Kombination der Optionen *CURVED* und *UPWARD* zu berücksichtigen. Diese Kombination erlaubt die Simulation mit beliebigem Einfallswinkel des Primärteilchens einschließlich des streifenden Einfalls, wobei die horizontale Schauerachse jede Höhe über dem Beobachtungsniveau einnehmen kann. In diesem Bericht wird die Wirkungsweise der Kombination der Optionen *CURVED*, *UPWARD* und *SLANT* des Luftschauersimulationsprogramms CORSIKA beschrieben. Die *SLANT*-Option kann mit allen anderen Optionen kombiniert werden und definiert für die Longitudinalentwicklung die Eindringtiefe des Schauers entlang der Schauerachse als *slant depth*, unabhängig von der Richtung des Primärteilchens.

Contents

1	Introduction	5
2	Geometry Definitions	6
2.1	UPWARD Option	6
2.2	Combined UPWARD & CURVED Options	7
2.3	Skimming Incidence	8
3	Routines for the SLANT Option	10
3.1	Modified Routines	10
3.1.1	Subroutine <i>COORIN</i>	10
3.1.2	Subroutine <i>COOINC</i>	10
3.2	New Routines for SLANT	11
3.2.1	Subroutine <i>DL2DT</i>	12
3.2.2	Subroutine <i>DT2DL</i>	15
3.2.3	Function <i>DISTAND</i>	16
3.2.4	Function <i>HEIGHTD</i>	16
3.2.5	Function <i>RADIUS0</i>	17
3.2.6	Function <i>DEPTH0</i>	17
3.2.7	Function <i>GAMMQ</i> and Subroutines <i>GCF</i> and <i>GSER</i>	17
3.3	Modifications of Binning Routines	17
3.3.1	Function <i>LBIN</i>	17
3.3.2	Function <i>THCKSI</i>	17
4	Longitudinal Tables	18
5	Example	19
5.1	Input	20
5.2	Output	20
	References	23

1 Introduction

Around the year 1990 the standard version of the air shower simulation program CORSIKA [1] has been designed for showers with nearly vertical incidence as observed by the KASCADE experiment [2] where the main interest is concentrated on the particles arriving at the detector level. In the meantime CORSIKA has become a widespread program for the simulation of Extensive Air Shower (EAS) experiments requiring partly very different geometry of incidence and observation: For the detection of showers induced by ultra-high energy (UHE) neutrinos with Earth skimming incidence at the Pierre Auger Observatory [3] (after horizontal penetration through the Andes mountains in West-East direction) or even by upward going neutrinos with observation from space in satellite experiments like EUSO [4] or OWL [5].

To meet the simulation needs of these experiments extensions to the possible directions of incidence¹ of the primary particle which induces the air shower were implemented. We discriminate different angular ranges of incidence and cover those ranges by program options which are presently (version CORSIKA 6.501) available.

- Downward moving primaries from vertical to moderate inclination in the zenith angle range $0^\circ \leq \theta \leq 60^\circ$. In this range the atmosphere is well approximated by layers with horizontal boundaries and the curvature of the Earth surface may be neglected. This range is well simulated using simple and fast algorithms and needs no selection of special CORSIKA options.
- Downward moving primaries within the zenith angle range $60^\circ \leq \theta < 90^\circ$. In this range the atmospheric layer boundaries have to follow the Earth curvature and the treatment is performed by a ‘sliding planar atmosphere’ [6] which is applied when selecting the *CURVED* option. The rotation of the coordinate frame from one locally planar section to the next one needs additional computing time and increases the simulation time. Upward scattered particles are discarded (but they are kept, if *CURVED* is combined with *UPWARD*).
- Skimming incidence with horizontal shower axis above the detector plane without reaching the Earth surface with $\theta = 90^\circ$. Special care has to be taken to avoid the division by the $\cos(\theta)$ which will become zero. The minimal altitude (apex) of the horizontal shower axis is specified by the input parameter HIMPCT (keyword *IMPACT*). Downstream the apex point the particles are moving upward, therefore for skimming incidence the *CURVED* option has to be combined with the *UPWARD* option.
- Upward moving primaries within the angular range $90^\circ < \theta \leq 120^\circ$. Such showers might be produced by neutrinos penetrating through the Earth and interacting close to the point where they leave the surface of the Earth rim again. For the

¹The zenith angle θ is here defined as the angle with the vertical at the (horizontal) detector plane.

simulation of those events the options *CURVED* and *UPWARD* must be combined. It is assumed that the detector level is high up, by technical reasons just below the top of atmosphere (which is at 112.8 km for the U.S. standard atmosphere).

- Upward moving particle close to the vertical direction $120^\circ \leq \theta \leq 180^\circ$. For those cases the Earth curvature may be disregarded and the simulation is simplified if only the *UPWARD* option is selected. Again the detector position has to be assumed just below the top of the atmospheric model.

In the standard version of CORSIKA, the longitudinal development as e.g. needed for the simulation of the fluorescence emission² is calculated in the vertical depth scale. This scale is not appropriate any more for highly inclined or even horizontal showers. The *SLANT* option uses instead the penetrated slant depth along the shower axis. Necessarily the *SLANT* option has to be programmed in a manner that a combination with all options needed to cover the full angular range of the primary particle is possible. This requirement needed a considerable modification and update of the existing code (version CORSIKA 6.200) described in Ref. [10].

2 Geometry Definitions

2.1 UPWARD Option

The geometry and the quantities which are necessary for the *UPWARD* option in combination with the *SLANT* option are explained in Fig. 1. The shower starts with the zenith angle θ above ground at the lower right corner and moving upwards reaches the observation level which is situated just below the top of atmosphere at the upper left corner. Drawn as short lines are some of the planes perpendicular to the inclined shower axis. As the atmospheric density decreases with increasing altitude, the distances between the tilted planes which mark the depth bins with equal penetrated matter thickness are increasing with increasing distance from the shower starting point. For each tilted plane i its altitude $H_{LONG}(i)$ at the crossing with the shower axis is kept in an array (and printed as table) as well as the distance $R_{LONG}(i)$ from the starting point and the corresponding penetrated slant depth $THCKRL(i)$. The index counting of these arrays starts at the starting point of the shower.

In the standard CORSIKA (without any option) the origin of the coordinate \mathbf{h} (altitude) is at sea level, while the origin of the horizontal coordinates \mathbf{x} and \mathbf{y} is defined by the point of first interaction³. To detect the passage of a particle through the tilted

²This emission is detected by the fluorescence telescopes of the Pierre Auger observatory [3], the HiRes [7], the Fly's Eye [8], or the Telescope Array [9] experiments.

³The coordinate origin is placed at the starting point of the primary particle (at the top of the atmosphere) if `TMARGIN` is set `.true.` by the input keyword `TSTART`.

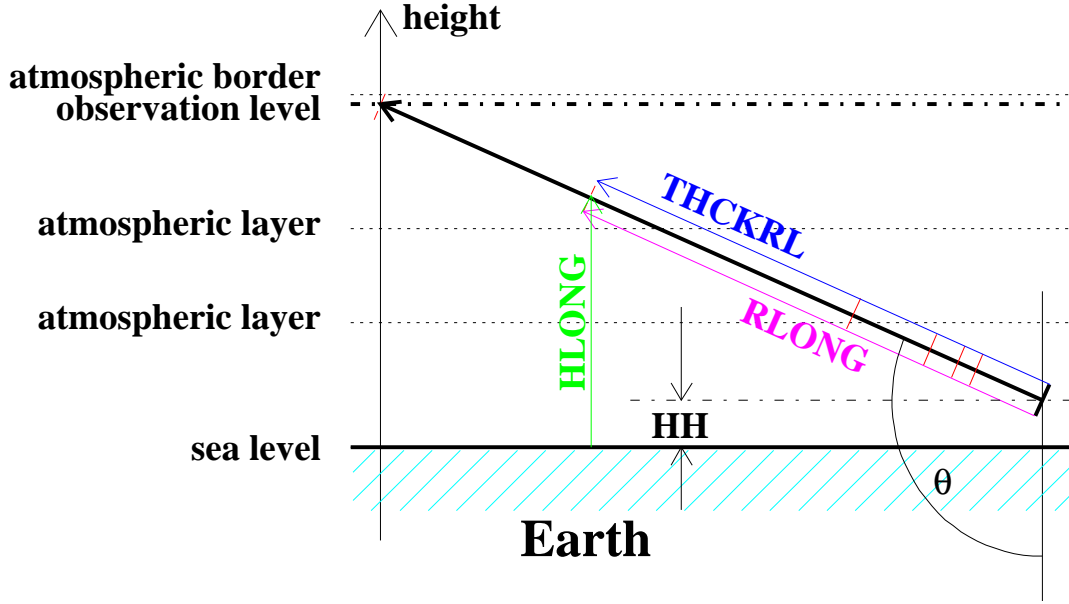


Figure 1: Geometry definitions of slant thickness in planar atmosphere.

plane i , its slant path along the shower axis

$$r = x \cdot \sin(\theta) \cdot \cos(\phi) + y \cdot \sin(\theta) \cdot \sin(\phi) - h \cdot \cos(\theta) + r_{\text{Loff}} \quad (1)$$

before and after the transport step must fulfill the condition

$$r_{\text{before}} < \text{RLONG}(i) < r_{\text{after}} \quad . \quad (2)$$

The angles θ and ϕ are the zenith and azimuth angles of the primary particle. The offset r_{Loff} is calculated from the condition that the primary particle at the starting point must fulfill Eq. (1) with $r = 0$, $x = 0$, and $y = 0$, which gives

$$r_{\text{Loff}} = h \cdot \cos(\theta) \quad .$$

The products $\sin(\theta) \cdot \cos(\phi)$ and $\sin(\theta) \cdot \sin(\phi)$ depend only on the primary's direction and are constants for a shower (denoted in the program by STHCPH and STHSPH).

2.2 Combined UPWARD & CURVED Options

When combining the *SLANT* option with the *CURVED* option or with both *CURVED* & *UPWARD* options the geometry is different and we have to consider the particle position in the Cartesian coordinate system of the detector. For an upward going shower within this system the zenith angle θ^* becomes $> 90^\circ$. Fig. 2 shows this situation. The altitude of the starting point (to be defined by the keywords FIXHEI or FIXCHI in the CORSIKA input file) and the position of the observation level (at the atmospheric border for an upward going shower) define the straight path length DIAG . The apparent

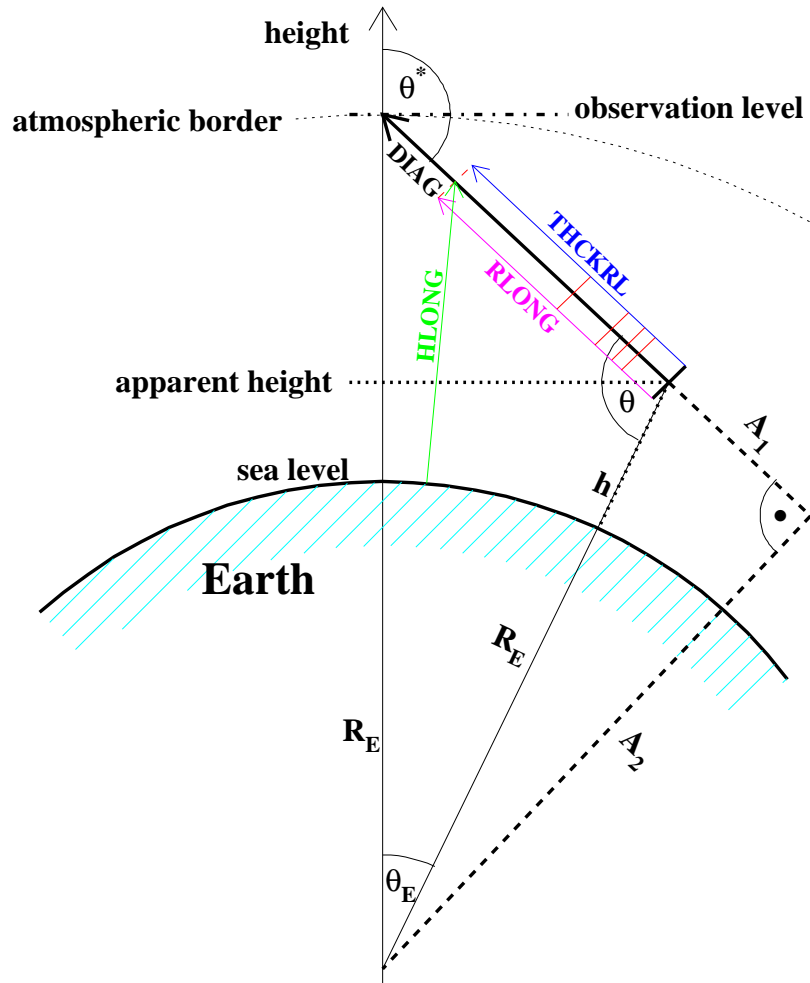


Figure 2: Geometry definitions in curved atmosphere for an upward going shower.

height is used as altitude, while the coordinate origin of the transverse coordinates \mathbf{x} and \mathbf{y} is taken at the point where the shower axis hits the observation level. The shower axis extends along the space diagonal **DIAG** which defines the angles θ^* and ϕ at the observation plane. The offset r_{Loff} is calculated in a manner that the slant path \mathbf{r} of Eq. (1) becomes zero at the shower starting point.

2.3 Skimming Incidence

At skimming incidence the horizontal shower axis is defined by the minimum altitude **HIMPCT** which is read in from the input with the keyword **IMPACT**. This special case is treated with a combination of the *CURVED* and *UPWARD* options. In Fig. 3 this

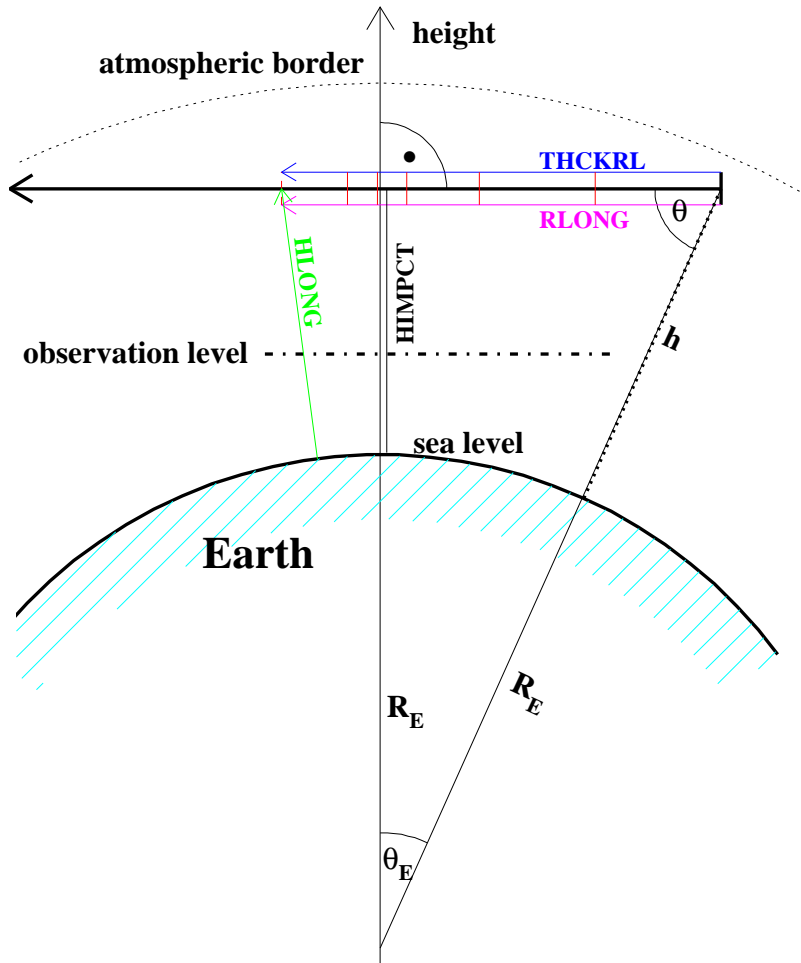


Figure 3: Geometry definitions in curved atmosphere for a skimming shower.

situation is sketched. Again the altitude \mathbf{h} of the starting point is given with the keywords `FIXHEI` or `FIXCHI` in the `CORSIKA` input file or is taken as the atmospheric border. For the calculation of the total slant depth between the starting point and the point where the shower axis leaves the atmosphere, the path is divided in two portions which are separated by the point of minimum altitude. For both segments a call to the new subroutine `DL2DT` (see Sect. 3.2.1) is performed within the subroutine `COINC`. Taking the origin of the Cartesian coordinates \mathbf{x} and \mathbf{y} at the point of minimum altitude, the offset distance $r_{L,off}$ used in Eq. (1) is calculated as before in a manner that the penetrated path length and matter thickness become zero at the shower starting point.

3 Routines for the SLANT Option

Several routines in CORSIKA were added for calculations which are necessary to get the longitudinal shower development along the slant depth. They are described in the following subsections. Moreover the routines *COORIN* (standard version) resp. *COOINC* (*CURVED* option) contain longer program blocks which deal with the initialization of the necessary arrays of $HLONG(i)$, $RLONG(i)$, and $THCKRL(i)$.

3.1 Modified Routines

3.1.1 Subroutine *COORIN*

In the standard version of CORSIKA (no options selected except *SLANT*), the additional programming of subroutine *COORIN* calculates the offsets in x and y for each observation level ⁴ in a manner that by the corrections $x - x_{\text{off}}$ resp. $y - y_{\text{off}}$ the coordinates refer to the crossing point of the shower axis through the considered observation level. In the standard CORSIKA version (no options selected except *SLANT*) the additional programming calculates the distance offset r_{Loff} and the constants $STHCPH$, $STHSPH$ which keep the primary's angles (see Sect. 2.1). The bin width $THSTEP$ specified by the keyword `LONGI` defines the penetrated thickness bin boundaries

$$THCKRL(i) = i \cdot THSTEP$$

and is used to get the values of the $HLONG$ array with the help of the function *HEIGH* (which gives the height value for a specified mass overlay)

$$HLONG(i) = HEIGH(i \cdot THSTEP \cdot \cos(\theta)) .$$

Finally the array $RLONG$ is calculated using the geometrical relation of the starting altitude HH and the actual altitude $HLONG$ by

$$RLONG(i) = (HH - HLONG(i)) / \cos(\theta) .$$

Special care is taken for those particles which travel off the shower axis and hit the observation level far away on the downstream side after passing the coordinate origin. Their energy deposit is collected in a last energy deposit bin which extends from the last but one bin to twice the total depth considered along the shower axis.

3.1.2 Subroutine *COOINC*

For the *CURVED* option [6] the routine *COOINC* performs essentially those calculations which are done by the subroutine *COORIN* in the standard version. For the *SLANT* option all initializing calculations depend on the direction of the primary particle (see topic 2 to 4 in Sect. 1). After calculating the total path length $DIAG$ along the

⁴Without the *CURVED* option several observation levels may be defined.

shower axis from geometric relations (see Ref. [6]) the call to the new routine *DL2DT* determines the total penetration thickness. For skimming incidence this subroutine is called twice, once to determine the downward path from the starting point to the lowest point of the shower axis, and a second time for the upward path from the lowest point to the exit out of atmosphere. Both sections are summed up to form the total penetrated thickness.

At present (version 6.501) the longitudinal tables comprise 1825 bins at maximum. For a skimming incidence with an impact altitude close to sea level the total penetrated thickness extends over $\approx 73000 \text{ g/cm}^2$. If the step length *THSTEP* was selected smaller than $73000/1825 \text{ g/cm}^2 = 40 \text{ g/cm}^2$, *THSTEP* is adjusted automatically to a suitable integer value to cover the full penetrated thickness at the given size of the longitudinal arrays. Finally the bin number, altitude, penetrated thickness, and penetrated slant path (calculated with routine *DT2DL*) at the bin boundaries are printed in a table which corresponds in its length with the size of the tables of longitudinal distributions (see the example of Sect. 5.2).

3.2 New Routines for SLANT

The new routines are needed if the option *SLANT* is combined with *CURVED* resp. with *CURVED & UPWARD*. They have been taken from the CONEX program [12] and adapted to the CORSIKA code. They comprise the routines *DL2DT*, *DT2DL*, *RADIUS0*, *DEPTH0*, *DISTAND*, and *HEIGHTD* [12, 13]. The routines *DL2DT* and *DT2DL* are called from the routine *COOINC* (see Sect. 3.1.2). The interdependence of the other routines and functions is visible in Fig. 4.

To explain the new routines we define a particle path which passes the Earth (with radius \mathbf{R}_E) in a distance \mathbf{a} from the middle, see Fig. 5. The starting point at an altitude \mathbf{h} above sea level has a distance \mathbf{z} to the lowest point (apex) of the path. Let us consider the traversed matter after reaching the point with distance \mathbf{z}_1 to the apex and with the altitude \mathbf{h}_1 as shown in Fig. 6. This traversed matter is given by the integral over the density along the path between \mathbf{z} and \mathbf{z}_1 . The variable ζ is the geometric length along the particle trajectory. As the density ρ itself is altitude dependent, we write the traversed matter $\mathbf{T}(\mathbf{z}_1)$ ⁵ by the integral

$$\mathbf{T}(\mathbf{z}_1) = \int_{\mathbf{z}}^{\mathbf{z}_1} \rho(\mathbf{h}(\zeta)) d\zeta . \quad (3)$$

In differential form it is written to

$$\frac{d\zeta}{d\mathbf{T}} = \frac{1}{\rho(\mathbf{h}(\zeta))} . \quad (4)$$

For the altitude dependence of the density within one layer of the atmosphere we assume $\rho(\mathbf{h}) = e^{[\mathbf{c}-\mathbf{b}\cdot\mathbf{h}]}$ with the atmospheric constants \mathbf{b} and \mathbf{c} . The ζ dependence of the

⁵We denote the depth by \mathbf{T} to be close to the notation of the program code. Probably x_{slant} would be better suited for this quantity.

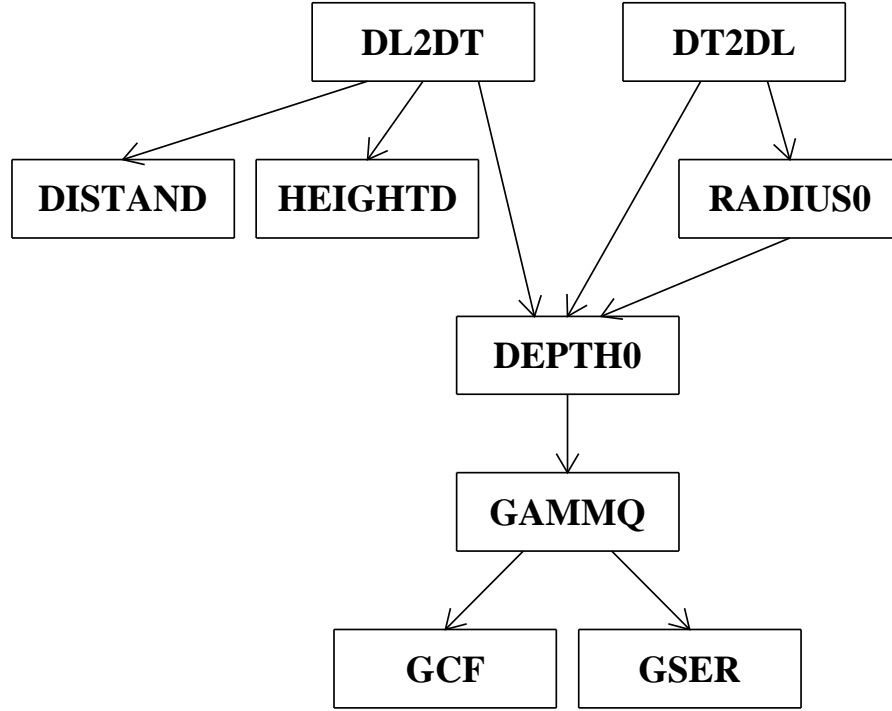


Figure 4: Hierarchy of the new subroutines and functions.

altitude h is expressed by the geometrical relation $R = \sqrt{\zeta^2 + a^2}$ to

$$h(\zeta) = \sqrt{\zeta^2 + a^2} - R_E \quad (5)$$

which results in

$$\rho(\zeta) = e^{[c - b \cdot (\sqrt{\zeta^2 + a^2} - R_E)]} . \quad (6)$$

3.2.1 Subroutine *DL2DT*

Within one layer of the the atmosphere the subroutine *DL2DT* converts the path length z to the traversed slant depth T . Using relation Eq. (6) we rewrite Eq. (3) to

$$T(z_1) = \int_z^{z_1} \exp \left[c - b \cdot \sqrt{\zeta^2 + a^2} - R_E \right] d\zeta . \quad (7)$$

For a multi-layered atmosphere the integral is replaced by a sum over several integrals fitting together at the integral boundaries and with individual atmospheric constants b and c according to the layer under consideration.

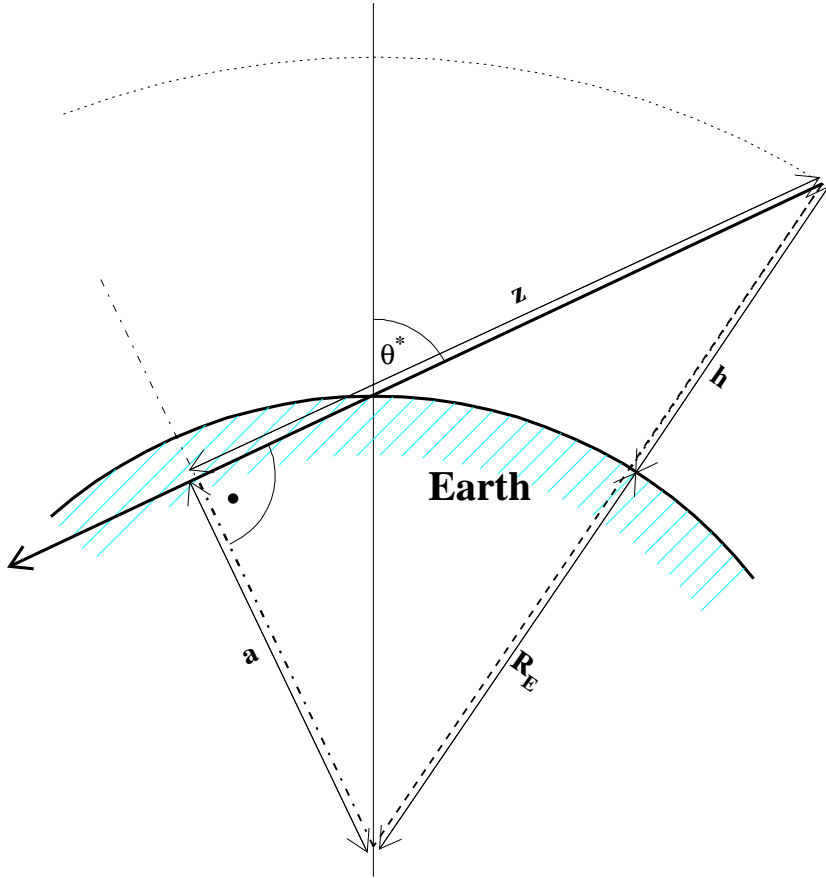


Figure 5: Trajectory with parameter $a < R_E$.

To solve this integral, we consider the altitude difference Δh between the trajectory points with distance ζ and with distance z_1 , using the relation Eq. (5) and considering that the Earth's radius cancels out:

$$\Delta h = h(\zeta) - h(z_1) = \sqrt{\zeta^2 + a^2} - \sqrt{z_1^2 + a^2} .$$

Taking $R_1 = \sqrt{z_1^2 + a^2}$ as factor before the bracket (because of better numerical stability) we get

$$\Delta h = R_1 \cdot \left\{ \sqrt{\frac{a^2 + \zeta^2}{R_1^2} - 1} \right\} . \quad (8)$$

If we denote $\Delta\zeta = \zeta - z_1$ we may rewrite Eq. (8) as

$$\Delta h = R_1 \cdot \left\{ \sqrt{\frac{a^2 + (z_1 + \Delta\zeta)^2}{R_1^2} - 1} \right\}$$

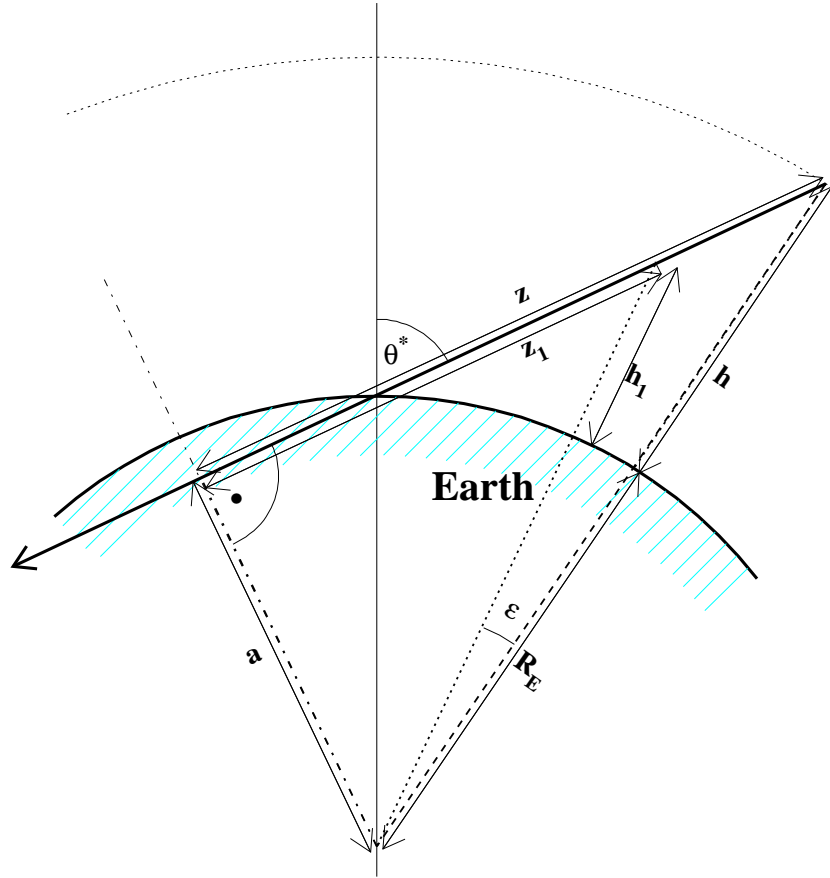


Figure 6: Particle moving on trajectory with parameter $a < R_E$.

which simplifies to

$$\Delta h = R_1 \cdot \left\{ \sqrt{1 + \frac{2z_1 \Delta \zeta + \Delta \zeta^2}{R_1^2}} - 1 \right\} . \quad (9)$$

As R_1 is always larger than $R_E \approx 6400$ km and the step size $\Delta \zeta$ is less than or of the order of the atmospheric thickness of ≈ 100 km, the fraction under the square root of Eq. (9) becomes

$$\frac{2z_1 \Delta \zeta + \Delta \zeta^2}{R_1^2} \ll 1$$

which permits a series expansion of the root of Eq. (9) with breaking after the linear term to get

$$\Delta h \simeq \frac{\Delta \zeta}{2R_1} (2z_1 + \Delta \zeta) .$$

With this expression we rewrite Eq. (7) extracting the ζ -independent expressions as factor before the integral and respecting $d\zeta = d\Delta\zeta$

$$T(z_1) \simeq \exp[c - b(R_1 - R_E)] \int_z^{z_1} \exp\left[-\frac{2bz_1\Delta\zeta + b\Delta\zeta^2}{2R_1}\right] d\Delta\zeta .$$

This integral can be solved analytically

$$T(z_1) \simeq \exp[c - b(R_1 - R_E)] \exp(bz_1^2/R_1) \left[\operatorname{Erf}\left(\sqrt{\frac{bz_1^2}{2R_1}}\right) - \operatorname{Erf}\left(\sqrt{\frac{bz_1^2}{2R_1}}\right) \right]$$

where $\operatorname{Erf}(z)$ stands for the error function

$$\operatorname{Erf}(z) = \int_0^z e^{-\Delta\zeta^2} d\Delta\zeta .$$

3.2.2 Subroutine *DT2DL*

The subroutine *DT2DL* converts the traversed slant depth \mathbf{T} to the path length \mathbf{z} . The problem to be solved is just the inverse of the preceding subsection. We start from Eq. (4) and replace ρ by Eq. (6)

$$\frac{d\zeta}{dT} = \exp\left[b(\sqrt{\zeta^2 + a^2} - R_E) - c\right] . \quad (10)$$

Replacing ζ by the distance to the center of the Earth one has to consider the dependence

$$\frac{dR}{d\zeta} = \sqrt{1 - a^2/R^2}$$

to get from Eq. (10) the relation

$$\frac{dR}{dT} = \frac{dR}{d\zeta} \cdot \frac{d\zeta}{dT} = \sqrt{1 - a^2/R^2} \cdot \exp[b(R - R_E) - c] . \quad (11)$$

We now consider that $\sqrt{1 - a^2/R^2} > \sin \varepsilon$, if the angle between the radial distances $R = R_E + h$ and $R_1 = R_E + h_1$ is denoted by ε (see Fig. 6). This angle ε reaches its maximum for skimming incidence close to ground with ($a \simeq R_E$) with the relation

$$\cos \varepsilon_{\max} = \frac{R_E}{R_E + h_{\max}}$$

where h_{\max} is the thickness of the atmosphere. As we are in the atmosphere, the condition $R_1 \geq R_E$ holds. The values of $R_E \approx 6400$ km and $h_{\max} \approx 100$ km result in a maximum value of $\varepsilon_{\max} \approx 10.1^\circ$, corresponding with $\sin \varepsilon_{\max} \approx 0.17$.

For values of ε with $\varepsilon \rightarrow \varepsilon_{\max}$ the right hand side of Eq. (11) becomes

$$\sqrt{1 - a^2/R^2} \simeq \sqrt{1 - a^2/R_1^2} .$$

Therefore we rewrite Eq. (11) by integration between z and z_1 considering that the right hand side does not depend on z

$$\int_R^{R_1} \exp[c - b(R - R_E)] \cdot dR \simeq \sqrt{1 - a^2/R_1^2} \cdot (T_1 - T)$$

which gives (with $\Delta T = T_1 - T$)

$$R(\Delta T) \simeq R_E + \left\{ c - \log \left[e^{c - b(R_1 - R_E)} - b \Delta T \sqrt{1 - a^2/R_1^2} \right] \right\} / b .$$

For a shower particle traversing the matter thickness ΔT starting from point z the transport distance Δz is given approximately by $\Delta z = z_1 - z$ with $z_1 = \sqrt{R^2(\Delta T) - a^2}$. Therefore the true distance Δz_{true} which corresponds with the matter thickness ΔT is not very different from ΔT ($|\Delta z_{\text{true}} - \Delta z| = |\delta z| \ll \Delta z$). The distance δz is not precisely known, but certainly much smaller than Δz and that corresponds with the matter thickness $\delta T = \Delta T - \Delta T_0$ where ΔT is the matter thickness between z and z_{true} and ΔT_0 is the matter thickness between z and z_1 . ΔT_0 may be calculated with the method of the previous Subsect. 3.2.1. Now starting at a new point z (close to z_1) and the matter thickness δT (close to ΔT) and moving from z_1 to z_{true} one may find again an approximate solution closer to the exact value, as now the transport step is smaller and $\sin \epsilon$ changes less along the step. This procedure is repeated until the desired precision is attained.

For values of ϵ with $\epsilon \rightarrow 0$ the approximate solution is found in a different manner. Starting from Eq. (10) for very small steps we have $\sqrt{z^2 + a^2} = R \simeq R_1$ which permits to write

$$\frac{dz}{dT} = \exp[b(R_1 - R_E) - c]$$

(constant density approximation). By integration we get

$$\Delta z = z_1 - z = \exp[b(R_1 - R_E) - c] \Delta T$$

with $\Delta T = T_1 - T$. As defined above we take a Δz which is only slightly different from Δz_{true} ($|\Delta z_{\text{true}} - \Delta z| = |\delta z| \ll \Delta z$). A more precise solution is attained in an iterative procedure like in the first case with $\epsilon \rightarrow \epsilon_{\text{max}}$.

An ϵ_{lim} may be found such that for $\epsilon > \epsilon_{\text{lim}}$ the first method and for $\epsilon < \epsilon_{\text{lim}}$ the second method is the more adequate solution with the better convergence.

3.2.3 Function *DISTAND*

The function *DISTAND* calculates the slant distance from a point with altitude \mathbf{h} to the observation level along a path with the impact radius \mathbf{a} (see Fig. 5).

3.2.4 Function *HEIGHTD*

The function *HEIGHTD* calculates the height \mathbf{h} (above sea level) for a point along a path with impact radius \mathbf{a} at a given distance from the observation level (see Fig. 5).

3.2.5 Function *RADIUS0*

The function *RADIUS0* calculates the radial distance to the center of Earth for the ending point of a path with impact parameter **a** and a slant depth interval from a starting point with given radius.

3.2.6 Function *DEPTH0*

The function *DEPTH0* calculates the slant depth interval between two points with given radius to the center of Earth along a path with impact parameter **a**.

3.2.7 Function *GAMMQ* and Subroutines *GCF* and *GSER*

The function *GAMMQ* determines the gamma function. In dependence on the argument X the steering function *GAMMQ* selects calls to the subroutines *GCF* (for $X > 1.5$) or *GSER* (for $X \leq 1.5$) to determine the value of the gamma function. The subroutine *GCF* uses the continued fraction representation of the incomplete gamma function $Q(A, X)$ with $A = 1/2$, while *GSER* uses the series representation of the incomplete gamma function $P(A, X)$ with $A = 1/2$, taking finally its complement to $1 - P(A, X)$.

3.3 Modifications of Binning Routines

3.3.1 Function *LBIN*

For given particle coordinates the function *LBIN* determines the longitudinal bin number of the particle position. An additional argument gives the lowest bin number which is used as starting value for the sequential search with increasing bin numbers. The modifications concern the arguments of the *LBIN* function. With the *CURVED* option the *LBIN* function is called now with the particle altitude *HAPP* relative to the detector plane. The transverse coordinates X and Y transmitted to the *LBIN* function are now calculated in the Cartesian system centered at the detector middle to get the appropriate slant depth bin number. This slant depth of each individual particle corresponds with the projection of the particle position onto the shower axis and taking the slant depth of the projection.

3.3.2 Function *THCKSI*

The function *THCKSI* determines the penetrated mass thickness for a given total path length along the shower axis. By a simple search algorithm applying the repeated bisectioning of the search interval the index j is determined for which *PATH1(j)* comes closest below the given path length. The final value of the penetrated matter is obtained by interpolating the table *TSLANT(j)* between j and $j + 1$ according to the increment of the table *PATH1(j)* in this index interval.

The update of this routine concerns the *CURVED* option. The particle coordinates are calculated in the Cartesian coordinate system centered in the middle of the detector to form the argument (slant depth path) for the call of the *THCKSI* function. In the previous CORSIKA version 6.204 the local coordinates have been used which are less appropriate with increasing zenith angle and increasing distance from the detector center.

4 Longitudinal Tables

In the CORSIKA printout file three longitudinal tables are available:

- 1) LONGITUDINAL PARTICLE DISTRIBUTION
- 2) LONGITUDINAL ENERGY DISTRIBUTION
- 3) LONGITUDINAL ENERGY DEPOSIT

The binning of Table 1) and 2) is characterized by the depth value of the inclined planes which form the bin boundaries.

The **first** table is incremented each time a particle is passing one of the horizontal (for the *SLANT* option tilted) planes which are separated by the matter thickness *THSTEP* (see Sect. 3.1.1). From the starting point at the depth *THICKH* a particle moves down (forward) to the end point at the depth *THCKHN* and crosses the planes with numbering *LPCT1*, *LPCT1 + 1*, ... *LPCT2* with *LPCT2 > LPCT1* (see Fig. 7).

The **second** table gives the energy content of each particle species along the longitudinal shower development. For charged particles the energy loss by ionization is taken into account, and it is assumed that during the transport the energy loss between the starting point and the end point is homogeneously distributed over the traversed matter between. Thus the energy loss per bin *EDEPB* is calculated

$$EDEPB = EDEP \cdot THSTEP / (THCKHN - THICKH)$$

where *EDEP* is the total energy loss along the path. The energy loss within the starting bin (between *LPCT1 - 1* and *LPCT1*) is calculated to

$$EDEP1 = EDEPB \cdot (THSTEP \cdot LPCT1 - THICKH) / THSTEP$$

and analogously the energy deposit *EDEPN* in the ending bin (between *LPCT2* and *LPCT2 + 1*) which only partially is penetrated by the particle. Using this energy loss the total particle energy at each crossing with a plane is well defined. For each plane all energies of a particle species are summed up in the second table.

With the **third** table the energy balance of the shower is established by summing up all bins of all particle species. For this table the energy deposit *EDEPB* (rsp. *EDEP1* or *EDEPN*) between the bin boundaries is summed up. Each bin is characterized by its depth value in the middle of the bin. In this table the deposit by ionization is separated from the deposit of particles which are discarded because of an energy or angular cut. For stable particles subject to cuts the kinetic energy at the cutting point is used, while

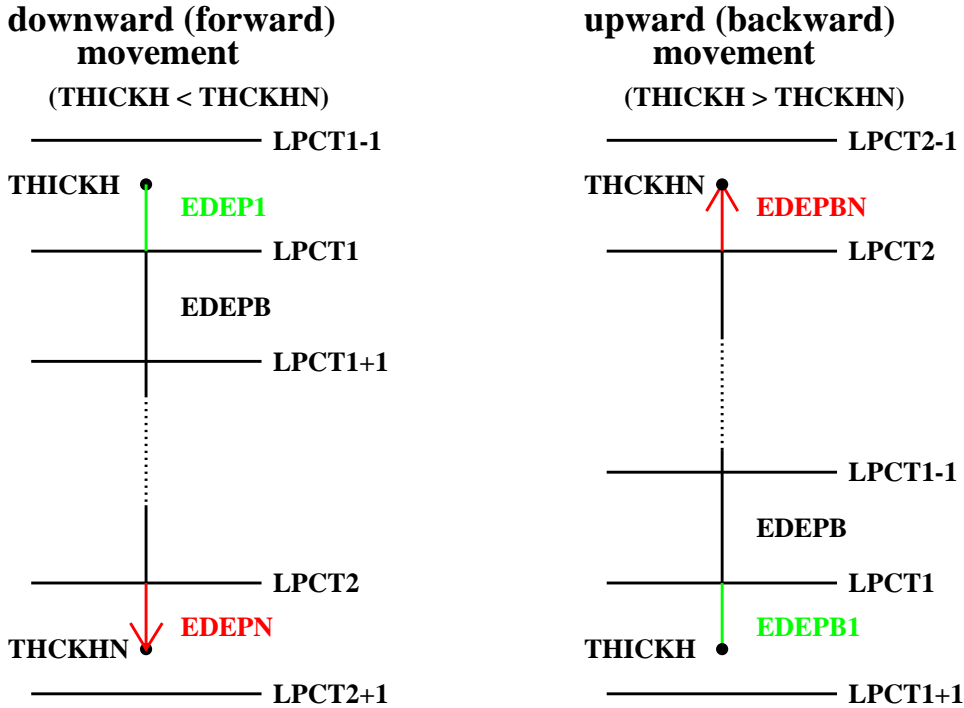


Figure 7: Numbering of longitudinal binning and energy deposit in the bins.

for antiparticles additionally two times the rest mass is added to account for possible annihilation [14]. For mesons the subsequent decay into neutrinos is respected by adding $3/4$ (for π^\pm and K^\pm) resp. $1/2$ (for $K_{S,L}^0$) of the total energy to the neutrino channel and the remainder energy to the hadron channel ⁶.

For upward moving particles (option *UPWARD*) resp. backward moving particles (option *SLANT*) the numbering of the bins is slightly different assuming $LPCT2 < LPCT1$, but the energy deposit calculations are performed analogously to the downward case. Details can be deduced from the right hand side of Fig. 7.

Using the *SLANT* option all the longitudinal output tables of CORSIKA refer to the *slant* depth along the shower axis instead of the *vertical* depth. This is indicated in the header lines of the longitudinal output tables for clear interpretation. All other features of the longitudinal tables are unchanged.

5 Example

This chapter gives an example of the application of the combined CORSIKA options *SLANT* with *CURVED* and *UPWARD*. The selection of these options is indicated at

⁶Implemented in CORSIKA versions 6.517 (July 2006) and later.

the beginning of the printout file (after the header) by the lines:

```
CURVED VERSION WITH SLIDING PLANAR ATMOSPHERE
=====
UPWARD VERSION FOR UPWARD GOING PARTICLES
=====
SLANT DEPTH FOR LONGITUDINAL DISTRIBUTIONS
=====
```

5.1 Input

In our example we regard a primary muon starting with a zenith angle of $\theta = 110^\circ$ at an altitude of ≈ 1400 m a.s.l. For the example run the specific command lines of the input file are used:

```
PRMPAR 5           primary mu(+)
ERANGE 1.0E+6 1.0E+6 primary energy
THETAP 110. 110.  upward zenith angle
FIXCHI 875.       start at depth 875 g/cm**2
OBSLEV 112828.00E2 observation at border of atmosphere
LONGI T 200. F T  longitudinal development every 200 g/cm**2
```

5.2 Output

In the printout file a table gives the connection between the altitude, the longitudinal bin borders, and the slant path length along the shower axis:

```
LONGITUDINAL SHOWER DEVELOPMENT:
SHOWER IS SAMPLED IN NSTEP = 15 SLANT STEPS OF 200.0 G/CM**2
STEP      HEIGHT [CM] SLANT DEPTH [G/CM**2] SLANT DISTANCE [CM]
(I)       HLONG(I)          THCKRL(I)          RLONG(I)
 0  140468.355482          0.000000          0.000000
 1  196942.185156          200.000000         192674.383570
 2  256876.686268          400.000000         396957.316107
 3  320724.010974          600.000000         614352.873772
 4  389031.162738          800.000000         846678.875167
 5  462399.322176         1000.000000        1095925.882667
 6  542488.127371         1200.000000        1367659.904009
 7  630747.286461         1400.000000        1666700.608027
 8  729032.741522         1600.000000        1999203.389360
 9  839927.753949         1800.000000        2373723.967004
10  967146.213713         2000.000000        2802541.266266
11 1116848.015903         2200.000000        3306013.169160
12 1312099.937799         2400.000000        3960856.445924
13 1596751.891625         2600.000000        4911879.828624
14 2130177.317823         2800.000000        6682590.717441
15 50000000.000000         3000.000000       130933662.194054
```


The tables of the longitudinal distributions in the print outout file (before the end of a shower) look like:

----- LONGITUDINAL PARTICLE DISTRIBUTION IN SLANT STEPS OF 200. G/CM**2 -----

DEPTH	GAMMAS	POSITRONS	ELECTRONS	MU+	MU-	HADRONS	CHARGED	NUCLEI	CHERENKOV
200.	9.	1.	1.	1.	0.	0.	3.	0.	0.00000E+00
400.	39.	3.	3.	1.	0.	0.	7.	0.	0.00000E+00
600.	1822.	100.	167.	1.	0.	0.	268.	0.	0.00000E+00
800.	700.	19.	33.	1.	0.	0.	53.	0.	0.00000E+00
1000.	548.	36.	38.	1.	0.	0.	75.	0.	0.00000E+00
1200.	509.	10.	23.	1.	0.	0.	34.	0.	0.00000E+00
1400.	95.	3.	3.	1.	0.	0.	7.	0.	0.00000E+00
1600.	45.	3.	0.	1.	0.	0.	4.	0.	0.00000E+00
1800.	39.	3.	4.	1.	0.	0.	8.	0.	0.00000E+00
2000.	54.	5.	5.	1.	0.	0.	11.	0.	0.00000E+00
2200.	264.	14.	20.	1.	0.	0.	35.	0.	0.00000E+00
2400.	248.	15.	28.	1.	0.	0.	44.	0.	0.00000E+00
2600.	108.	8.	13.	1.	0.	0.	22.	0.	0.00000E+00
2800.	105.	6.	7.	1.	0.	0.	14.	0.	0.00000E+00
3000.	129.	5.	7.	0.	0.	0.	12.	0.	0.00000E+00

----- LONGITUDINAL ENERGY DISTRIBUTION [GEV] IN SLANT STEPS OF 200. G/CM**2 -----

DEPTH	GAMMAS	POSITRONS	ELECTRONS	MU+	MU-	HADRONS	CHARGED	NUCLEI	SUM
200.	1.18985E-01	8.75309E-02	9.71136E-03	9.99999E+05	0.00000E+00	0.00000E+00	9.99999E+05	0.00000E+00	9.99999E+05
400.	2.38148E+01	1.71923E+01	1.24186E+02	9.99831E+05	0.00000E+00	0.00000E+00	9.99972E+05	0.00000E+00	9.99996E+05
600.	6.24444E+01	1.64089E+01	1.96941E+01	9.99830E+05	0.00000E+00	0.00000E+00	9.99866E+05	0.00000E+00	9.99928E+05
800.	1.08271E+01	8.49454E-01	8.80972E-01	9.99826E+05	0.00000E+00	0.00000E+00	9.99828E+05	0.00000E+00	9.99839E+05
1000.	4.99551E+01	7.21808E+00	3.05562E+00	9.99755E+05	0.00000E+00	0.00000E+00	9.99765E+05	0.00000E+00	9.99815E+05
1200.	1.11922E+01	2.04559E+00	2.40355E+00	9.99754E+05	0.00000E+00	0.00000E+00	9.99759E+05	0.00000E+00	9.99770E+05
1400.	1.18766E+00	3.93213E-02	9.96070E-02	9.99753E+05	0.00000E+00	0.00000E+00	9.99753E+05	0.00000E+00	9.99754E+05
1600.	8.93305E-01	3.90935E-01	0.00000E+00	9.99750E+05	0.00000E+00	0.00000E+00	9.99751E+05	0.00000E+00	9.99752E+05
1800.	9.08719E-01	1.25853E-01	8.02702E-01	9.99746E+05	0.00000E+00	0.00000E+00	9.99747E+05	0.00000E+00	9.99748E+05
2000.	1.60506E+00	8.32753E+00	1.78600E+00	9.99732E+05	0.00000E+00	0.00000E+00	9.99742E+05	0.00000E+00	9.99744E+05
2200.	6.02811E+00	1.31544E+00	7.67155E-01	9.99722E+05	0.00000E+00	0.00000E+00	9.99724E+05	0.00000E+00	9.99730E+05
2400.	4.77497E+00	9.42031E-01	2.01841E+00	9.99709E+05	0.00000E+00	0.00000E+00	9.99712E+05	0.00000E+00	9.99716E+05
2600.	4.89280E+00	1.67318E+00	4.40618E+00	9.99696E+05	0.00000E+00	0.00000E+00	9.99703E+05	0.00000E+00	9.99707E+05
2800.	1.42042E+00	4.45162E-01	3.41056E-01	9.99695E+05	0.00000E+00	0.00000E+00	9.99696E+05	0.00000E+00	9.99698E+05
3000.	4.61090E+00	2.96957E-01	2.95879E-03	0.00000E+00	0.00000E+00	0.00000E+00	2.99916E-01	0.00000E+00	4.91081E+00

----- LONGITUDINAL ENERGY DEPOSIT [GEV] IN SLANT STEPS OF 200. G/CM**2 -----

DEPTH	GAMMA	EM IONIZ	EM CUT	MU IONIZ	MU CUT	HADR IONIZ	HADR CUT	NEUTRINO	SUM
100.0	0.0	0.1	0.0	1.1	0.0	0.0	0.0	0.0	1.1
300.0	0.0	1.6	0.1	1.1	0.0	0.0	0.0	0.0	2.7

500.0	0.7	61.9	4.1	1.1	0.0	0.0	0.0	0.0	67.8
700.0	1.4	79.8	6.7	1.1	0.0	0.0	0.1	0.0	89.0
900.0	0.4	20.4	1.7	1.1	0.0	0.0	0.0	0.0	23.6
1100.0	0.6	40.9	3.1	1.1	0.0	0.0	0.0	0.0	45.6
1300.0	0.3	12.9	1.2	1.1	0.0	0.0	0.0	0.0	15.4
1500.0	0.0	1.6	0.1	1.1	0.0	0.0	0.0	0.0	2.9
1700.0	0.0	2.5	0.2	1.1	0.0	0.0	0.1	0.0	3.9
1900.0	0.0	2.3	0.2	1.1	0.0	0.0	0.0	0.0	3.6
2100.0	0.2	11.6	0.8	1.1	0.0	0.0	0.0	0.0	13.6
2300.0	0.2	11.8	0.9	1.1	0.0	0.0	0.0	0.0	14.0
2500.0	0.1	7.2	0.6	1.1	0.0	0.0	0.0	0.0	9.0
2700.0	0.1	7.8	0.6	1.1	0.0	0.0	0.0	0.0	9.6
2900.0	4.7	3.9	1.4	1.4	999686.2	0.0	0.1	0.1	999697.8
3100.0	0.00000E+00	0.00000E+00	0.00000E+00	0.00000E+00	0.00000E+00	0.00000E+00	0.00000E+00	0.00000E+00	0.00000E+00
LONGITUDINAL ENERGY SUM [GEV]									
0.87551E+01	0.26628E+03	0.21691E+02	0.16378E+02	0.99969E+06	0.00000E+00	0.23644E+00	0.10627E+00		
0.0	0.0	0.0	0.0	0.0	0.0	0.0	0.0		
ENERGY SUM = 9.999964E+05 GEV									

With the command lines of Sect. 5.1 a muon of 1 PeV starts at 875 g/cm² (corresponding with 1405 m a.s.l.) and moves upward with an inclination angle of 70° (zenith angle 110°). The first interaction takes place at an altitude of 1932 m (mass overlay 820 g/cm²) and produces by Bremsstrahlung and pair production several electromagnetic particles, which form an upward em-shower. The muon loses only a very small fraction of its energy in these interactions. Such interactions take place several times before the muon arrives at the dummy 'observation level' just below the border of the atmosphere. The energy content of the muon may be followed in the output table 'LONGITUDINAL ENERGY DISTRIBUTION' which gives the energy content within each particle species. The energy balance at the end of the 'LONGITUDINAL ENERGY DEPOSIT' table demonstrates the energy conservation within the precision of the shower calculation which e.g. neglects the rest mass of the primary muon of 0.105 GeV. It is worth to notice that at the muon energy of ≈ 1 PeV the ionization energy loss of ≈ 5.5 MeV/(g cm⁻²) (resulting in a deposit of 1.1 GeV per bin of 200 g/cm² thickness) is much higher than the minimum ionization energy loss of 2.2 MeV/(g cm⁻²) at low energies.

Acknowledgements: I thank my colleague T. Pierog for the fruitful collaboration in the development of the CORSIKA program. I am indebted to R. Engel for many suggestions and carefully reading the manuscript.

References

- [1] D. Heck et al., *CORSIKA: A Monte Carlo Code to Simulate Extensive Air Showers*, Report **FZKA 6019**, Forschungszentrum Karlsruhe, 1998; http://www-ik.fzk.de/corsika/physics_description/corsika_phys.html
- [2] T. Antoni et al., KASCADE Collaboration, *Nucl. Instr. Meth. A* **513** (2003) 490
- [3] AUGER Collaboration, J. Abraham et al., *Nucl. Instr. Meth. A* **523** (2004) 50
- [4] M. Pallavicini for the EUSO Collaboration, *Nucl. Instr. Meth. A* **502** (2003) 155; A. Petrolini for the EUSO Collaboration, *Nucl. Phys. B* (Proc. Suppl.) **113** (2002) 329; O. Catalano, *Il Nuovo Cimento* **24C** (2001) 445; <http://www.euso-mission.org/>
- [5] F.W. Stecker et al., *Nucl. Phys. B* (Proc. Suppl.) **136** (2004) 433; <http://owl.gsfc.nasa.gov/>
- [6] D. Heck, *The CURVED Version of the Air Shower Simulation Program CORSIKA*, Report **FZKA 6954**, Forschungszentrum Karlsruhe, 2004; <http://www-ik.fzk.de/~heck/publications>
- [7] T. Abu-Zayyad et al., *Nucl. Instr. Meth. A* **450** (2000) 253
- [8] R.M. Baltrusaitis et al., *Nucl. Instr. Meth. A* **240** (1985) 410
- [9] M. Sasaki, Proc. of the EHECR 2001, Report **ICRR-481-2001-11**, Inst. Cosmic Ray Research, Tokyo, 2001; <http://www-ta.icrr.u-tokuo.ac.jp>
- [10] D. Heck, *The SLANT Option of the Air Shower Simulation Program CORSIKA*, Report **FZKA 7082**, Forschungszentrum Karlsruhe, 2004; <http://www-ik.fzk.de/~heck/publications>
- [11] D. Heck and T. Pierog, *CORSIKA User's Guide*, Forschungszentrum Karlsruhe; http://www-ik.fzk.de/corsika/usersguide/corsika_tech.html
- [12] T. Pierog et al., Proc. **29th Int. Cos. Ray Conf.**, 2005, Pune (India), **7**, 103; T. Pierog et al., *Nucl. Phys. B* (Proc. Suppl.) **151** (2006) 159
- [13] V. Chernatkin, *Simulation des gerbes dues aux rayons cosmiques à très hautes énergies*, Thèse Université de Nantes (France), 2006
- [14] M. Risse and D. Heck, *Astrop. Phys.* **20** (2004) 661